Action Spectrum and Quantum Efficiency for Proton Pumping in *Halobacterium halobium*†

R. A. Bogomolni,* R. A. Baker, R. H. Lozier, and W. Stoeckenius

ABSTRACT: The action spectrum and quantum efficiency (ϕ_{H^+}) for proton ejection from *Halobacterium halobium* have been determined under conditions chosen to minimize light-triggered proton influx which is usually observed in intact cells. The action spectrum for the carotenoid-containing strain, R_1, shows that light energy absorbed by the carotenoids does not contribute to the proton ejection. After correction for shielding by the carotenoids and other cell pigments, the action spectrum closely follows the absorption spectrum of bacteriorhodopsin. Values determined for ϕ_{H^+} in *H. halobium* cells and cell envelopes range from 0.4 to 0.7. These values are significantly higher than the currently accepted value for the quantum efficiency for the photoreaction cycle of bacteriorhodopsin in isolated purple membrane, suggesting that at least in intact cells and envelopes more than one proton is pumped during the bacteriorhodopsin photocycle. A new nondestructive assay for bacteriorhodopsin in intact cells and envelopes which also contain other pigments was used in this work.

The purple membrane of *Halobacterium halobium* functions as a light-driven proton pump which ejects protons from the cell (Oesterhelt & Stoeckenius, 1973), generating a proton concentration gradient and an electric potential across the cell membrane. Light-generated protonmotive forces of up to 300 mV have been measured in cell suspensions (Belyakova et al., 1975; Bogomolni et al., 1976a,b; Bakker et al., 1976; Bogomolni, 1977) and in model systems (Kayushin & Skulachev, 1974; Renthal & Lanyi, 1976; Michel & Oesterhelt, 1976; Drachev et al., 1977; Hwang & Stoeckenius, 1977).

Bacteriorhodopsin (bR), the retinal-containing chromoprotein which comprises ~75% of the purple membrane mass, is the energy converter. It exists in a metastable, "light-adapted" form absorbing maximally at 568 nm (bR_{568}^{LA}) and a stable, "dark-adapted" form absorbing maximally at 558 nm (bR_{558}^{DA}). bR_{568}^{LA} undergoes a light-induced reaction cycle (Lozier et al., 1975; Dencher & Wilms, 1975) which is accompanied by a release of protons from the exterior surface of the membrane and an uptake at the cytoplasmic surface (Lozier et al., 1976). The quantum efficiency for this photochemical cycle, ϕ_c, has been studied by several groups under different conditions and with different assumptions. Values reported for ϕ_c range from ~0.03 (Kung et al., 1975) to 0.79 (Oesterhelt & Hess, 1973), with recently reported values near 0.3 (Goldschmidt et al., 1977; Lozier & Niederberger, 1977; Becher & Ebrey, 1977). In isolated purple membrane fragments reported stoichiometries of protonation changes per bacteriorhodopsin molecule cycling (S_{H^+}) range from $S_{H^+} \leq 1$ in water (Lozier et al., 1976; Hess et al., 1978) to ~3 at high ionic strength (Hess et al., 1978). The quantum yield for proton release was found to increase from 0.25 to 0.43 as ionic strength is increased, with no change in the quantum yield for the photochemical cycle (Ort & Parson, 1979). Obviously the stoichiometry of H^+ translocated/bacteriorhodopsin molecule cycling ($S_{\vec{H}^+}$) must be measured in oriented closed systems. It has been suggested that some protons may be released and rebound from the same side of the membrane (Bohr protons) (Eisenbach et al., 1978). Although photocycling and proton pumping have been demonstrated in oriented systems [Lozier et al., 1976; for a detailed review of measurements by several groups, see Stoeckenius et al. (1979)], the stoichiometry has not been determined. The quantum efficiency for proton translocation should, of course, be equal to the product of ϕ_c and $S_{\vec{H}^+}$. However, it is possible that one or both of these factors varies with the conditions of the measurement. Oesterhelt & Krippahl (1973) estimated 0.3–0.5 proton pumped per photon absorbed by an indirect method, i.e., the inhibition of respiration by light. Their calculation required the assumption that inhibition of respiration is tightly coupled to the light-driven proton pump and that the H^+/O_2 ratio of 12 reported for mitochondria pertains. Later measurements by Belyakova et al. (1975) support the latter assumption. We have reported a preliminary value of $\phi_{H^+} = 0.7 \pm 0.2$ obtained in intact cells by direct measurements of light-driven proton efflux (Bogomolni et al., 1976b). Recent reports of the pumping efficiency for phloretin-treated cells by Oesterhelt's group (Hartmann et al., 1977) are in good agreement with our preliminary value. Measurements in intact cells are complicated by light-triggered proton influxes (Bogomolni et al., 1976a). We report here a direct measurement of the quantum efficiency for proton pumping in *H. halobium* cells under conditions which minimize the light-triggered proton inflow (Bogomolni et al., 1976a) either by discharging the preexisting proton electrochemical potential across the membrane or by blocking the inflow through the ATPase with DCCD.[1] We have also used isolated cell envelopes where it is easier to manipulate the dark electrochemical gradients, but these preparations suffer from defects of the permeability barrier and/or inverted orientation of a part of the pigment.

Materials and Methods

Cell and Cell Envelope Preparations. H. halobium R_1, a carotenoid-containing mutant lacking vacuoles, was grown on complex medium consisting of "basal salt" solution (4.27 M NaCl, 0.027 M KCl, 0.081 M $MgSO_4$, and 0.018 M $CaCl_2$) supplemented with Oxoid peptone L-37 (1% w/v), 1.1×10^{-6} M $MnSO_4$, and 1.8×10^{-5} M $FeCl_2$. Starter cultures were inoculated from slants into 50 mL of medium in 250-mL flasks

† From the Cardiovascular Research Institute and Department of Biochemistry and Biophysics, University of California, San Francisco, California 94143. *Received July 3, 1979; revised manuscript received December 10, 1979.* This work was supported in part by NASA Grant NSG-7151, National Heart and Lung Institute Program Project Grant HL-06285, National Science Foundation Grant 76-11801, and National Institutes of Health Grant GM23651.

[1] Abbreviations used: CCCP, carbonyl cyanide *m*-chlorophenylhydrazone; DCCD, *N,N'*-dicyclohexylcarbodiimide; CTAB, cetyltrimethylammonium bromide.

0006-2960/80/0419-2152$01.00/0

and grown for 3 days at 37 °C on a rotary shaker operated at 150 rpm. Twenty-milliliter aliquots of the starter were used for inoculation of 2-L flasks containing 700 mL of medium. The cultures were incubated at 37 °C in the rotary shaker and illuminated with four 40-W fluorescent lamps placed ~50 cm above the flasks. Cells containing reduced amounts of bacteriorhodopsin were grown with increased aeration and/or lower illumination intensity (Oesterhelt & Stoeckenius, 1973). After 3 to 4 days the cells were harvested by centrifugation, washed twice in basal salts, and resuspended in basal salt solution to a final concentration of 1.1–1.2 mg of cell protein per mL (5×10^9 cells/mL). Protein was measured with the biuret technique with bovine serum albumin as a standard. Cell counts were obtained in a Petroff-Hauser counting chamber. Cell lysis was measured by monitoring the absorbance of supernatants at 260 or 280 nm after separating the cells from the medium by centrifugation and/or by the menadione reductase activity in the cell suspension (Lanyi & MacDonald, 1976). Cell suspensions with more than 5% lysis were rejected. pH was adjusted by addition of 0.1 M HCl or NaOH as required.

Cell envelope vesicles prepared according to MacDonald & Lanyi (1975) were provided by Dr. J. K. Lanyi. Envelopes were washed once before use in 4 M NaCl solution and resuspended in 3 M KCl to a final protein concentration of 1.5 mg/mL. The pH was not adjusted and typically stabilized at ~6.6. Misorientation and/or leakiness of the preparation was determined by the menadione reductase assay (Lanyi & MacDonald, 1976).

Ferrioxalate actinometer solutions were prepared by following standard procedures (Hatchard & Parker, 1956; Lee & Seliger, 1964). All handling of potassium ferrioxalate was done under deep red safelights. Acid and bases were standardized against potassium phthalate and/or potassium bicarbonate as primary standards. Commercially available analytical reagent chemicals from various sources were used without further purification.

Instrumentation. Proton release and light absorption by *H. halobium* cells and cell envelopes were measured in a cylindrical acrylic plastic chamber of our own construction. The chamber has a 15-mm optical path length and a 16-mm diameter and is provided with a water jacket. The device is completely transparent. An opening at the top admits a semimicrocombination pH electrode (Beckman Instruments No. 39003). A Teflon-coated magnetic stirring bar at the bottom rapidly stirs the sample, and a circulating thermostated water bath connected to the water jacket controls the temperature to within ±0.5 °C. The pH electrode and the stirring bar are positioned just above and below the light path, respectively. The space between the electrode stem and the top opening wall permits addition of reagents with calibrated microsyringes (Hamilton 7000 series). Limited gas exchange occurs due to the imperfect seal, leaving the cell suspensions under semianaerobic conditions; in some experiments nitrogen gas was blown over the chamber top to achieve complete anaerobicity. The measuring chamber was positioned at the center of an integrating sphere (a gift from C. S. French) which could be split into halves. During the measurements of light-induced pH changes, the sphere remained open to admit the thermostat tubing, the pH electrode, and the shaft of the stirrer. The pH electrode signal was fed into an electrometer amplifier (Keithley 610 C) or to a pH meter (Instrumentation Laboratory Model 135A) and the amplified signal recorded with a high-speed two-channel Clevite-Brush Mark 280. The system time response to an acid pulse was 0.2 s, and the sensitivity was ~0.001 pH unit.

The time scale for all measurements was given by the time marker of the recorder, which is line frequency controlled. A prefocused 300-W arc lamp (General Electric Marc 300) collimated with appropriate lenses (one located within the integrating sphere), filtered through 5 cm of water, a dichroic heat reflecting filter (Optical Industries, Inc.), and a Corning 1-75 infrared-absorbing filter illuminated the sample. Monochromatic radiation was obtained with interference filters (Baird Atomic) for quantum efficiency measurements or with a Bausch & Lomb high-intensity monochromator for action spectra. Illumination times were controlled with electromagnetic shutters and light intensities with calibrated neutral density filters. For the measurement of the cell suspension transmittance, the pH electrode and the water lines were removed and replaced by white Teflon plugs, the sphere was closed, and the actinic beam, attenuated with neutral density filters, was used as the measuring beam. This procedure minimizes the problem of varying geometric parameters such as path lengths and internal reflections because the measuring and actinic beams are identical except for intensity.

Absorption spectra were obtained with a single-beam integrating sphere spectrophotometer of our own design and construction. The light source is a compact filament tungsten halogen lamp powered by a highly stable dc power supply (Lambda LE103FM). The filament is focused onto the entrance slit of a 0.25-m monochromator (Jarrell Ash 82-410) equipped with a stepper motor wavelength-scanning drive (Jarrell Ash 82-462). A cutoff filter (Corning 3-69) is used above 600 nm to reject second-order stray light. The output beam from the monochromator is collimated and deflected upward by a mirror into an integrating sphere (30-cm diameter) through a 1-cm^2 hole onto a 2.5-cm diameter, 1-cm path length, cylindrical cuvette positioned at the center of the sphere. With this vertical light path the sample remains in the measuring beam even if settling of the sample onto the front window of the cuvette occurs. The photodectector (EMI 9659QA photomultiplier in a Pacific Photometric Model 62 housing) is protected from direct reflections by a baffle plate. The photomultiplier output is fed into a logarithmic current-to-voltage converter (Analog Devices 755P), digitized with a Nicolet SD-71B A-to-D converter, and stored in a signal-averaging computer (Nicolet 1074). A small light source and photodiode which bracket a perforated metal disk attached to the scanning mechanism synchronize the computer with the wavelength of the monochromator. The position of the order-sorting filter is determined by a rotary solenoid controlled by the computer. After the single-beam spectrum of the sample is measured and stored in core memory, the sample is replaced by basal salt and its spectrum is also scanned and stored. The difference between the sample and blank yields the absorption spectrum in optical density units. Spectra are permanently stored on magnetic tape (Kennedy 9700) and plotted with an X-Y recorder.

Measuring Techniques. We have to measure two parameters: (a) the initial rate of proton release into the suspension medium, $R_{[H^+]}$, and (b) the constant rate (einsteins per second) of photon capture by the pumping chromophore

$$R_{h\nu}^{\,i} = I_0(1 - T)f_i \tag{1}$$

where I_0 is the total incident light flux in einsteins per second, T is the transmittance of the sample, and f_i is the fraction of absorbed light captured by the pumping chromophore i (i.e., bR) defined by

$$f_i = A_i/\Sigma A_j \tag{2}$$

where $\sum A_j$ includes all chromophores absorbing at a given wavelength. For action spectroscopy only the relative incident quantum flux vs. actinic wavelength and $R_{[H^+]}$ must be known.

(*a*) *Initial Rate of Proton Release.* Cell suspensions were prepared for measurements by adjusting the pH and adding the indicated reagents; typically the samples required ~30 min for stabilization. Then light-induced pH changes were recorded for several light intensities. At the beginning and at the end of the experiment several acid and base pulses were used to determine the buffering capacity of the system:

$$B = \Delta[H^+]/\Delta pH \tag{3}$$

The pulses were adjusted to elicit pH changes up to as large as the maximum observed light-induced changes in order to check the linearity of ΔpH vs. $\Delta[H^+]$ in the pH range of the experiment. Initial slopes of the light-induced changes were determined graphically by positioning a mirror perpendicular to a ruler at the time origin. The initial rates (gram-ions of H^+ per second) of proton ejection were then calculated from

$$R_{[H^+]} = B\left(\frac{\Delta pH}{\Delta t}\right)_{t=0} \tag{4}$$

(*b*) *Measurement of Light Absorption.* To determine the absolute rate of light absorption by bR, $R_{h\nu}^{bR}$, we must measure (1) the incident light flux, (2) the fraction of the incident light flux absorbed by the sample, and (3) the fraction of the absorbed radiation captured by bR.

(*1*) *Incident Light Flux.* We routinely began the experiments by determining the incident light flux with the ferrioxalate chemical actinometer (Hatchard & Parker, 1956; Lee & Seliger, 1964). The chamber, carefully washed and dried, was positioned in the sphere and filled with 3.2 mL of actinometer solution. The light source was allowed to stabilize before opening the shutter and illuminating the sample for 600 s through a 420-nm interference filter of 10-nm bandwidth. The light intensity and illumination period were recorded with a PIN photodiode (Hewlett-Packard 5082-4220) in the second channel of the recorder. (The same diode was used to monitor the light intensity during measurement of light-induced pH changes in cell suspensions.) An interference filter identical with that used in the main optical path was positioned in front of the photodiode to avoid artifacts due to stray light since the lamp could not be completely enclosed. Although the sphere assembly was enclosed in a black cloth canopy, we checked for light leaks into the sphere by running with a closed shutter for the same time required for lamp warm-up and the measuring period. The measured leak equaled ±2% of the minimum light intensity used in the experiments, and that background was cancelled by subtracting the leak value from the actinic beam flux.

The actinometry had to be done at 420 nm and the quantum efficiency determinations at 575 nm. Therefore, at the end of the chemical actinometry a radiometer probe (Laboratory Data Control Div. Model 68 radiometer, Milton Roy Co.) calibrated against a standard filament lamp (National Bureau of Standards S-56) was positioned at the back window of the measuring chamber, the chamber was filled with water, and the incident light powers with the 575- and 420-nm filters were determined. Flatness of response of the radiometer was checked by comparing its response to that of a thermopile (Charles M. Reeder and Co., Detroit, MI) over the wavelength range 400–750 nm. The light source for this comparison was a 250-W tungsten Halogen lamp, and the Bausch & Lomb high-intensity monochromator was operated with a 5-nm bandwidth. The second-order spectrum was rejected above 600 nm with a 3-68 Corning filter. The maximum discrepancy between detectors was less than 5% from 400 to 750 nm.

Although the chemical actinometer with the revised quantum yields of Lee & Seliger (1964) was our primary standard, we checked the actinometer against the calibration of the National Bureau of Standards lamp. For this purpose a well collimated light beam was passed through the 420-nm interference filter and then diverged onto an opal glass. The intensity of light behind the opal glass was tested for homogeneity by positioning the thermopile at several points. An area of 1 ± 0.05 cm^2 was screened with black photographic tape, and chemical actinometry values for this assembly were compared with the calibrated thermopile and radiometer readings. The maximum absolute discrepancy observed was ~8%.

The total incident photon flux (einsteins per second) at 575 nm was calculated from

$$I_0^{575} = \frac{M_{Fe^{II}} E^{420} P^{575/420}}{Q^{420} E^{575} \Delta t} \tag{5}$$

where $M_{Fe^{II}}$ is the moles of Fe^{II} produced in the chemical actinometer, $P^{575/420}$ is the ratio of incident light power at 575 vs. 420 nm determined with the radiometer, E^{575} and E^{420} are the energies per photon at 575 and 420 nm, respectively, Q^{420} is the quantum yield for the actinometer at 420 nm (Lee & Seliger, 1964), and Δt is the illumination time.

(*2*) *Light Absorbed by the Cell Suspension.* The fraction of the incident light absorbed by the cell suspension at the actinic wavelength was determined with the integrating sphere shown schematically in Figure 5. Since a lens was used inside the sphere to collimate the beam, part of the incident light is reflected onto the sphere walls and does not reach the sample but is collected by the photodetector. Therefore, a correction is necessary unless all of the reflections could be made to exit the sphere through the entrance opening. The beam geometry used prohibited this solution, and we purposely collected the reflections by very slightly tilting the lens and measuring chamber. The measured transmittance (uncorrected for reflections) was calculated from

$$T_{measd} = V_{sample}/V_{basal\ salts}$$

where V_{sample} and $V_{basal\ salts}$ are the voltages developed by the photodetector with the sample and basal salts, respectively, in the chamber. The corrected transmittance (see Appendix) is given by

$$T_{cor} = \frac{T_{measd} - nr}{1 - nr} \tag{6}$$

where n is the number of reflections and r is the reflection coefficient for the light. We used $r = 0.04$ for both glass and plexiglass since the error introduced is negligible for our detection sensitivity. The reflections at the front and back faces of the lens and at the front face of the chamber yield $n = 3$, and we ignore the weak reflection at the solid aqueous interface. Since T measured ≥0.63 in all of the experiments reported, this correction is ≤9%.

(*3*) *Fraction of Light Absorbed by bR.* To correct the quantum yield values and the action spectrum for shielding, we must determine the absorption spectrum of the sample and of the relevant pigments and calculate f_i. The strong scattering from the cell suspensions causes path length errors, sieve effects, and sloping base lines which complicate the measurement (Duysens, 1956). The spectra obtained with our single-beam integrating-sphere, scanning spectrophotometer are free of the sloping base line problem but may still be distorted by sieve and path length effects. For our purpose, however, it suffices

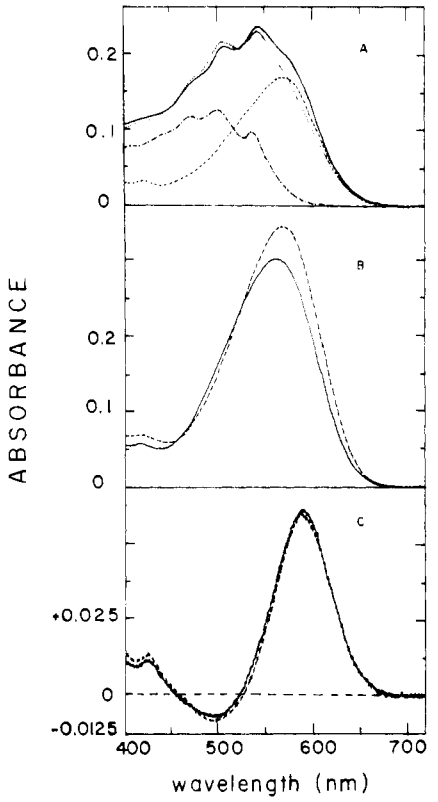

FIGURE 1: Light adaptation of bacteriorhodopsin in cell suspensions and in isolated purple membrane suspensions in basal salt. Spectra were taken with the integrating sphere at 23 °C, pH 7. (A) Absorption spectra of a cell suspension before (···) and after (—) light adaptation for 2 min with the tungsten source through a Corning 3-69 filter at a light intensity of 2×10^5 ergs/(cm^2 s). Absorption of bacteriorhodopsin calculated from the light–dark difference spectrum (- - -). Absorption of the cell suspension after subtraction of purple membrane absorption (–·–). (B) Absorption spectra of a purple membrane suspension in basal salt before (—) and after (- - -) light adaptation (illumination conditions as in part A). (C) Light minus dark difference spectra for the cells (- - -) and for the isolated purple membrane (—).

to obtain the fraction of the total measured absorbance due to bR. If it can be determined in the same sample by a nondestructive method which preserves the measuring geometry, these artifacts will cancel when the absorbance ratios are calculated. The spectral shift of the purple membrane absorbance toward longer wavelengths upon light adaptation (Becher & Cassim, 1976) was found to be a suitable nondestructive method for the in vivo determination of bR in the cell suspensions.

The difference in absorbance at any wavelength between the bR_{568}^{LA} and bR_{558}^{DA} can be used to quantitate the bacteriorhodopsin content by assuming that the difference spectrum between bR_{558}^{DA} and bR_{568}^{LA} is the same in cells and in isolated purple membrane in basal salt. To a good approximation, this was found to be true (see Figure 1). To determine the purple membrane concentration, we chose the wavelength 590 nm, where the difference in absorption between bR_{568}^{LA} and bR_{558}^{DA} is maximal. The absorbance increase at 590 nm upon light adaptation $\Delta A_{LA\text{-}DA}{}^{590}$ is 0.215 of the total absorbance of bR_{568}^{LA} at this wavelength. Thus, the absorbance at 590 nm of light-adapted bacteriorhodopsin in the intact cell at 590 nm is calculated simply from

$$A_{bR_{568}^{LA}}{}^{590} = \Delta A_{LA\text{-}DA}{}^{590}/0.215 \qquad (7)$$

This value assumes that the path length and sieve effects are the same in cells and isolated membrane. Although this is not expected to be exactly true, the error introduced by this assumption is probably small. The cell suspensions were light-adapted at 23 °C and pH 6 to 7 by illumination in a 1-cm path length cylindrical cuvette with a tungsten iodine source through a Corning 3-69 filter at a light intensity of 2×10^5 ergs/(cm^2 s) for 2 min. The spectrum of purple membrane in basal salt (Figure 1B) is scaled to the calculated absorbance at 590 nm and inserted into Figure 1A. From this spectrum we calculated f_{bR} at the actinic wavelength (575 nm) (see eq 3) as

$$f_{bR}{}^{575} = A_{bR}{}^{575}/A_{cells}{}^{575} \qquad (8)$$

where bR and the cells are in the light-adapted state. Values for $f_{bR}{}^{575}$ were greater than 0.75 and less than 1.0. We also compared this bR assay with the CTAB-bleaching assay in 13 different cell cultures, grown at conditions which provided a large range of purple membrane concentrations, to establish the accuracy of the light–dark purple membrane assay (Figure 2). For the calculation of the absolute purple membrane contents, we had to account for the effective optical path length of our cell suspensions. This we determined experimentally for the typical cell concentration used (5×10^9 cells/mL; 1.2 mg of cell protein per mL) as follows. The spectrum of a known amount of purple membrane was subtracted from the spectrum of the same amount of purple membrane added to a suspension of cells which contained no purple membrane detectable by the light-adaptation technique. The spectrum of the purple membrane in the cell suspension was obtained by subtraction of the spectrum of cells alone from that of the cells plus purple membrane. This calculated spectrum showed larger extinction than the pure purple membrane suspension. The increased absorbance (~20%) followed the shape of the purple membrane spectrum and was attributed to the increased path length due to light scatter.

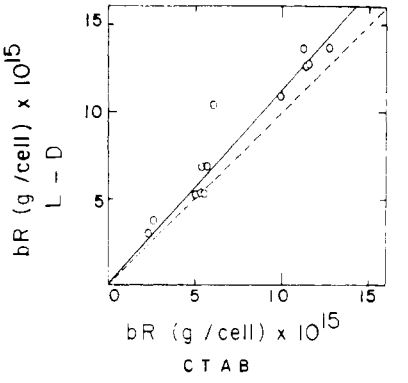

FIGURE 2: Bacteriorhodopsin content of cells assayed by the light–dark adaptation method vs. the CTAB-bleaching method. Values are calculated for an extinction coefficient at 570 nm of $\epsilon_{570} = 63\,000$ L mol^{-1} cm^{-1} and a molecular weight of 26 000. The effective path length for the light–dark adaptation method (cell concentrations 5×10^9 cells/mL) was 1.2 times the nominal cuvette value as determined experimentally (see text). Solid line: linear least-squares fit of straight line to data. Broken line: theoretical line. The difference may be due to losses during the isolation procedure required for the CTAB-bleaching method.

Results

Action Spectra. The bacteria used in these experiments contain in addition to bR other carotenoid pigments (Kelly et al., 1970). As action spectra show, similar carotenoid pigments are very efficient light energy collectors in chlorophyll-based photosynthesis (Rabinowitch, 1964). It is therefore important to determine whether or not light absorbed by the other carotenoids contributes to the light-driven process in *H. halobium*, especially the proton pumping of intact cells. If

bR is the only energy-converting pigment, as our preliminary data indicate (Stoeckenius et al., 1975), only the fraction of the incident radiation absorbed by bR should enter into the calculation of quantum yields.

Determination of action spectra requires a high degree of reproducibility during successive illuminations and careful exclusion of saturation effects. The light-induced pH changes of aerobic or anaerobic suspensions of *H. halobium* in basal salt solution are very reproducible at a given light intensity and initial pH. However, the pH changes are complex (Bogomolni et al., 1976a,b); influxes and effluxes occur simultaneously and are difficult to analyze. Varying the light intensity at a fixed wavelength shows that the proton efflux and proton inflow saturate at intensities differing by more than 1 order of magnitude (Bogomolni et al., 1976a). At very low intensities, where both influx and efflux would be free of saturation artifacts, the pH response is dominated by the influx and the uncertainty in the efflux kinetic parameters is too large for accurate determination of action spectra. We use experimental conditions designed to separate light-induced medium acidification (efflux) and alkalization (inflow). Only alkalization is observed at high pH, low light intensity, or low bacteriorhodopsin content. Acidification dominates under the inverse conditions. Alternatively, the proton inflow can be abolished by treatment of the cell suspensions with low concentrations of uncouplers, nigericin, and ATPase inhibitors such as DCCD or peliomycin (Bogomolni et al., 1976a). Illumination of the bacterial suspension under these conditions causes a prompt acidification, completely reversible in the dark, and the effect can be elicited reproducibly several times. Therefore, it is possible to measure initial rates of light-driven proton ejection into the suspending medium at different light fluxes. However, the action of the uncouplers and of nigericin does not persist for more than 1 or 2 h at such concentrations. While this period is sufficient to obtain the necessary data for a measurement of quantum yield for proton ejection, it is not long enough to measure an action spectrum accurately. Fortunately, DCCD has a longer lasting effect.

The action spectrum for proton pumping by bR, taking into account shielding by other pigments, should be determined by the fraction of photons absorbed by bR, $F(\lambda)$

$$F(\lambda) = \frac{I_a}{I_0} = (1 - T_{cells}(\lambda))A_{bR}(\lambda)/A_{cells}(\lambda) \qquad (9)$$

where I_a is the absorbed light intensity and the other parameters are defined above. The absorption spectra of the light- and dark-adapted cells, the scaled absorption of their purple membrane (calculated from the light minus dark difference spectrum as described under Materials and Methods), and the spectrum of the rest of the cell material obtained by subtracting the purple membrane from the whole cell spectrum are shown in Figure 1A. The action spectrum for proton ejection and the calculated fractional absorbance of the purple membrane in the absence and in the presence of shielding effects, $F(\lambda)$, are shown in Figure 3. The agreement between $F(\lambda)$ and the observed action spectrum indicates that no measurable energy transfer from the carotenoids to bR occurs, and therefore only the fraction of photons absorbed by purple membrane should be used in calculating quantum yields. The shielding effect is very small, as expected for an optically thin sample. In the low absorbance limit (<0.1 *A*), $F(\lambda) \simeq 1 - T_{bR}(\lambda)$. The action spectrum for proton pumping in the 400–430-nm region departs significantly from the calculated $F(\lambda)$. This discrepancy, if real, suggests that the photochemical quantum efficiency in that region is lower than that in the main absorption band.

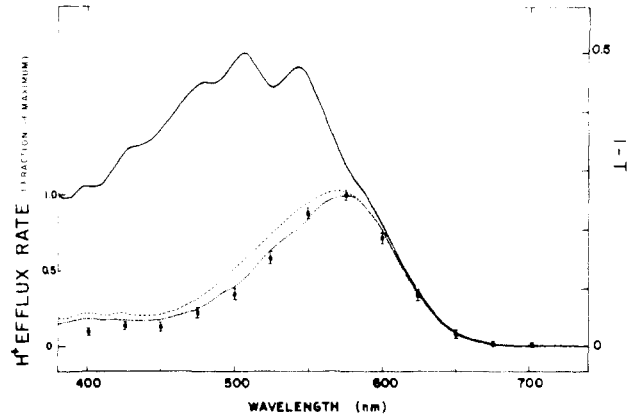

FIGURE 3: Action spectrum for initial proton pumping rates in a DCCD-treated cell suspension (cell concentration as in Figure 2). (---) Absorption of the purple membrane of the cells calculated from the light–dark difference spectrum in fractional absorption units ($1 - T$). (···) Absorption by the purple membrane taking shielding by the other chromophores into account [$F(\lambda)$]. (●) Action spectrum for $\Delta H^+/\Delta t$ at $t = 0$ expressed in arbitrary units and normalized to coincide at 575 nm with the corrected absorption trace. (—) Absorption of the cells in fractional absorption units ($1 - T$).

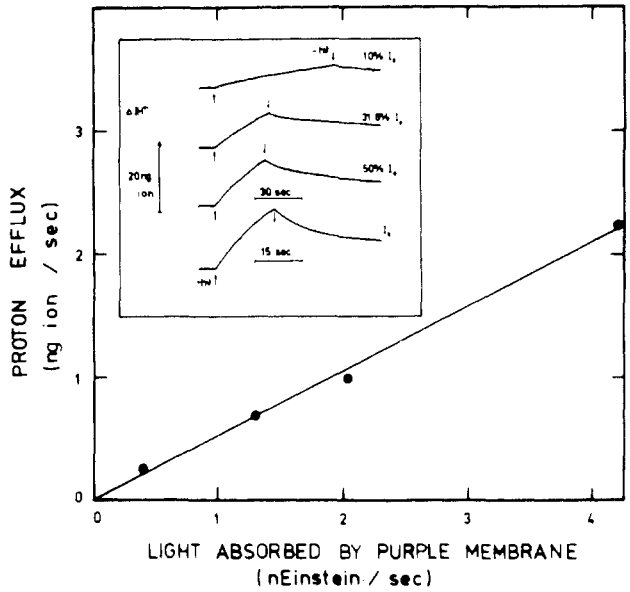

FIGURE 4: Quantum yield for proton pumping in nigericin-treated cells. Inset: light-induced proton concentration changes in a cell suspension containing 10^{-7} M nigericin. The illumination period is indicated by arrows. I_0 indicates the relative incident light intensity at 575 nm. Cell concentration 4.5×10^9 cells/mL (0.95 mg of protein per mL); pH 6.5; temperature 23 °C. The initial rates of proton ejection calculated from the data in the inset are plotted vs. light intensity. The quantum yield for this sample is $\phi_{H^+} = 0.52$ proton/photon absorbed.

This possibility would be more directly tested by determining the action spectrum for cycling in purple membrane. Photoreactions of intermediate M_{412}, which result in inhibition of pumping (Ormos et al., 1978), cannot explain the lower yields because the concentration of intermediate M_{412} in the photostationary state is negligible.

Quantum Yields. Figure 4 shows results from a typical experiment to determine initial rates of proton pumping as a function of light intensity. In this case nigericin was used to abolish the light-induced proton inflows. The inset shows the light-induced pH change in the medium for four different light intensities. We determined the initial rates of proton ejection as described under Materials and Methods. These rates are plotted as a function of the photon absorption rate. The

Table I: Quantum Yield for Light-Induced Proton Efflux

expt no.	sample	additions	pH	quantum yield (proton/photon)
1	cells	none	5.2	0.45 ± 0.05
2	cells	10^{-7} M nigericin	6.6	0.79 ± 0.11[e,f]
3[a]	cells	10^{-7} M nigericin	6.5	0.52 ± 0.05[e]
4[a]	cells	10^{-7} M nigericin	6.4	0.64 ± 0.06[e]
5[a]	cells	10^{-6} M CCCP	6.7	0.44 ± 0.04
6	cells	10^{-4} M DCCD	6.9[b]	0.59 ± 0.05
7[a]	cells	10^{-4} M DCCD	6.7[c]	0.40 ± 0.05
8A	envelope vesicles	none	6.6	0.58 ± 0.08
8B	envelope vesicles	10^{-4} M DCCD	6.6	(0.71)[d]

[a] Experiments 3 and 5 as well as 4 and 7 are pairs done sequentially on aliquots of the same cell stock with the same standardized acid solutions using the same actinometry value. [b] Strictly anaerobic sample. [c] Semiaerobic cells. [d] In experiment 8B, 10^{-4} M DCCD was added to the envelope vesicle suspension used in experiment 8A. This treatment resulted in a 15% increase in the initial pumping rate and a 7% increase in buffering capacity, giving an overall 22% increase in ϕ_{H^+}. Acid used for calibration pulses for both experiments as well as the actinometry and transmittance is the same. Therefore, the uncertainty is very small and the difference between experiments 8A and 8B is significant. [e] Weighted mean value of experiments 2, 3, and 4 and its standard deviation calculated according to Bevington (1969) is 0.59 ± 0.07 proton/photon. [f] Note that in this early experiment the error is unusually large because of excesive noise in the transmittance measurement.

quantum yield in this experiment was 0.52 proton/photon.

Table I summarizes our measurements of the quantum yield for proton ejection under different experimental conditions. The values reported in Table I are not corrected for the fraction of cells that are broken or leaky because this fraction is very small. The envelope vesicle preparations used here show only light-induced acidification so that the treatments used on whole cells are not necessary. They are, however, partly misoriented (Lozier et al., 1976) and/or leaky, as determined by the menadione reductase assay. The values reported with envelopes are not corrected for misorientation or leakiness because it is not known whether they are leaky or misoriented. The assumption that the menadione reductase value is due only to leaky vesicles would increase the quantum yield by ~20%.

Discussion

The differences in the observed quantum yields under different conditions are rather large with absolute values ranging from 0.40 to 0.79 proton/photon. Even under nearly identical conditions (experiments 2, 3, and 4 in Table I) values vary from 0.52 to 0.79 proton/photon.

Our uncertainty in the absolute calibration of light intensities is not larger than the 8% discrepancy between the accepted quantum efficiency of the chemical actinometer (Lee & Seliger, 1964) and our measurement based on the calibration of the National Bureau of Standards filament lamp. We have used the actinometry values as the primary standard for the calculations. Chemical actinometry errors were estimated by following Wraight & Clayton (1973). Statistics for the calibrating pulses of acid (or base) used to determine the buffering capacity gave standard deviations up to 8%. Other errors in our determination arise from the measurement of the transmittance (typically around 8%) and from the correction for the fraction of the total absorption which corresponds to bacteriorhodopsin (5%). Statistics were also done on initial slopes obtained at several light intensities. The combined error for the determination of quantum yield (square root of the sum of squares) is ~12%. The quantum yield values reported in Table I are the mean values and their standard deviations.

The rather large differences in ϕ_{H^+} values for different experiments are presumably due, at least in part, to differences in the state of the cells at the beginning of the experiment. Some of these differences may be rationalized in terms of the specific effects of the various agents on preexisting electrical and osmotic gradients and on the cells' energy metabolism. Halobacteria cells even in saline under anaerobic conditions in the dark are not readily depleted of their energy supplies, and for long periods they maintain ATP levels at ~30% of the level found in fully energized cells. ATPase inhibitors rapidly deplete this residual ATP, suggesting that it is sustained by continued synthesis (Hartmann & Oesterhelt, 1977; Danon & Caplan, 1976). The most likely driving force for this synthesis is the large potassium ion gradient, which in anaerobic cells in the dark slowly decays within 2 days (Bogomolni, 1977; Wagner & Oesterhelt, 1976). Resting cells as used in our experiments maintain an electric membrane potential of ~100 mV (Bakker et al., 1976; Michel & Oesterhelt, 1976; Bogomolni, 1977) which is largely, but not solely, determined by the K^+ diffusion potential (Wagner & Oesterhelt, 1976) and a pH gradient of ~2 pH units in a basal salt solution near pH 5. The pH gradient monotonically decreases with increasing extracellular pH, reaching zero at about pH 8. The decrease is largely compensated for by an increase of membrane potential which keeps the total electrochemical potential of protons, $\Delta\bar{\mu}_{H^+}$, nearly constant at $\Delta\bar{\mu}_{H^+}/nF \simeq 150$ mV. Illumination increases the membrane potential by 50 mV and triggers a substantial proton inflow so that only an alkalinization of the medium is observed initially. Agents which increase the proton permeability of the membrane abolish the triggered proton inflow and permit us to measure the light-driven proton ejection at level flow conditions. We have used the proton ionophore CCCP, which reduces $\Delta\bar{\mu}_{H^+}$, and nigericin, which mediates electroneutral proton-for-potassium exchange across the membrane. At low CCCP concentrations the increased proton permeability may still be overcome by the light-driven pump (Bogomolni et al., 1976a), but the CCCP experiments may give low apparent quantum yields because the increased proton permeability may affect the initial slope measurements and the ϕ_{H^+} values obtained should be considered lower limits. Nigericin causes a large proton uptake driven by the potassium gradient and has the advantage that the increased membrane potential generated by light cannot drive protons back into the cell through the electroneutral H^+/K^+ exchange mechanism.

Net proton inflow associated with ATP synthesis, which dominates the early pH changes under most conditions, can be reduced or abolished by treatment with DCCD or by lowering the medium pH to ~5 (Danon & Caplan, 1976; Oesterhelt, 1975; Bogomolni, 1977). Under these conditions, the preexisting electrochemical potential should not change much. Proton inflows coupled to other transport processes as well as passive leaks are still effective and the ϕ_{H^+} values obtained should also be considered as minimal values.

Envelope vesicles as used in our experiments should not have an electrochemical gradient in the dark; they are, however, rather permeable for protons, which is presumably caused by a damaged membrane ATPase. DCCD does indeed increase significantly the measured initial rate of proton ejection (Table I).

Envelope vesicles yield even higher values if we correct for leakiness or misorientation. Leakiness due to membrane damage may also affect our measurements in cell suspensions. While our discussion has obviously idealized the conditions

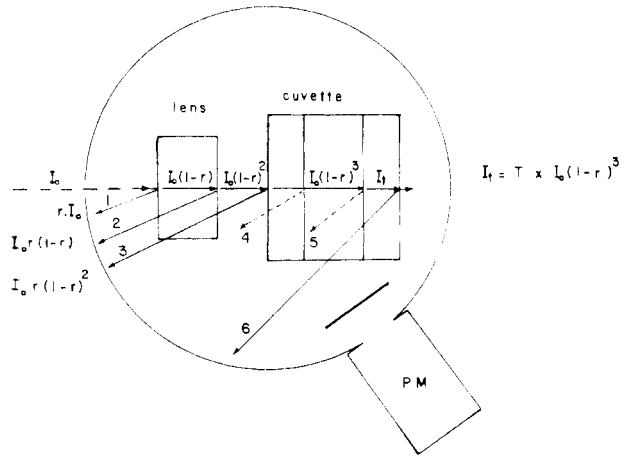

FIGURE 5: Reflections from the optical surfaces in the integrating sphere. To collect the reflections the chamber and lens are slightly tilted with respect to the incident beam. All reflections occurring before the sample, including the front wall of the cuvette, are collected by the photomultiplier without passing through the sample. This causes an error in the measured transmittance, T^m. The true transmittance, T, is given as shown in the Appendix.

to a considerable extent, it is difficult to see how we could have overestimated the initial rate of proton ejection and it appears likely that we have underestimated ϕ_{H^+} in most if not all our experiments.

Eisenbach et al. (1978) have claimed that in addition to protons pumped across the membrane, a significant number of protons also dissociate from the extracellular surface under illumination. The rate constant for this process is reported to be $\sim 0.2\ s^{-1}$. Such a process could contribute to the acidification of the extracellular medium for the initial 10–15 s of illumination only. In our quantum yield measurements on DCCD-treated cells and cell envelope vesicles we have not observed such a kinetic component. Both in DCCD-treated cells and in DCCD-treated vesicles the light-induced pH change rises linearly for almost 1 min. Obviously, in this case it makes no difference whether initial rates of proton release or rates averaged over 1 min are used in the calculation of yields. The pH changes in nigericin-treated cells at low intensities (Figure 4) as well as in cells at pH 5 are also dominated by single rise and decay components. Only in CCCP-treated cells and in untreated cell envelope vesicles did we observe a significant contribution of additional kinetic components with time constants in the range of a few seconds. For those samples, the maximal initial rates were used in the calculations and gave pumping yields comparable to those of samples not showing complex rise kinetics.

Rounded off to the nearest integer, the data in Table I indicate that two photons are needed to pump one proton, consistent with the quantum efficiency found by others for intact cells (Hartmann & Oesterhelt, 1977). Oesterhelt & Hess (1973) have reported a quantum yield for the photoreaction cycle of $\phi_c = 0.79$ for purple membrane in ether-saturated basal salt. This value combined with our largest proton-pumping efficiency values yields a pump stoichiometry of ~ 1 proton/cycle. All other investigators, however, measured ϕ_c values close to 0.3 in aqeous suspensions of purple membrane (Goldschmidt et al., 1976, 1977; Becher & Ebrey, 1977). Our own estimate of the maximum quantum yield obtained from photostationary state data of bacteriorhodopsin and its bathoproduct at 77 K is consistent with the lower value (Lozier & Neiderberger, 1977). We have recently experimentally compared the quantum yields obtained under the conditions used by Oesterhelt & Hess (1973) with those obtained under conditions where all other investigators reported values near 0.3. We found no difference and conclude that Oesterhelt & Hess are probably in error (Lozier et al., 1979). The value of $\phi_{H^+} = 0.6$ combined with $\phi_c = 0.3$ then leads to a stoichiometry of 2 pumped protons/photocycle. If we use our higher ϕ_{H^+} values and the lowest ϕ_c value, the stoichiometry would be even higher and approach 3.0.

The stoichiometry of net proton release and uptake by purple membrane suspensions has been discussed repeatedly. At low ionic strength one proton or less is released per molecule cycling. However, at higher ionic strengths higher values up to 3 have been reported (Hess et al., 1978; Ort & Parson, 1978). Obviously net proton release from membrane sheets is not necessarily a measure for pumped protons. However, taking $\phi_c = 0.3$, the present results indicate that two protons are pumped per molecule cycling in intact bacteria, suggesting that the 2 protons/cycle released in purple membranes at high ionic strength are pumped. Unfortunately, as long as the details of the photoreaction cycle have not been rigorously determined, all measurements of the proton stoichiometry, $S_{H^+} = \phi_H/\phi_c$, remain ambiguous because determinations of ϕ_c require assumptions about reaction pathways and extinction coefficients.

Added in Proof

During revision of this manuscript we measured the stoichiometry of proton pumping, $S_{\vec{H}^+}$, in envelope vesicles and in intact cells of *H. halobium* using *p*-nitrophenol absorbance changes as an indicator of proton concentration changes in the suspending medium (Lozier et al., 1976). Minimum values for the fraction of molecules photocycling were determined from the maximal transient absorbance decrease at 600 nm or the increase at 400 nm. Absorbance changes of the indicator dye were obtained by subtracting the absorbance change of matched buffered samples (0.01 M Hepes) from those of the unbuffered samples. We obtained $S_{\vec{H}^+} = 1.0 \pm 0.5$ $H^+/bR_{cycling}$. In cells the maximum value was $S_{\vec{H}^+} = 1.75 \pm 0.25$ $H^+/bR_{cycling}$. However, the decay of the dye absorbance change in cells is unexpectedly rapid ($t_{1/2} \sim 30$ ms), in contrast with the slow decay time in envelope vesicles (~ 10 s). The slow decay is consistent with the passive proton permeability of the envelope vesicles. The fast relaxation observed in cells indicates that other factors are contributing to the observed protonation changes. In fact, the dye signal in cells resembles that seen in suspensions of purple membrane fragments (Lozier et al., 1976).

Acknowledgments

We thank Lloyd Briggs for technical assistance and Jo Ann Ventura for the art work.

Appendix

Correction for Internal Reflections. As shown in Figure 5, the measured incident light $I_0^m(\lambda)$ at wavelength λ is

$$I_0^m(\lambda) = K(\lambda)rI_0[(1 - r) + (1 - r)^2 + \ldots + (1 - r)^n] = K(\lambda)rI_0\sum_1^n(1 - r)^n$$

where $I_0(\lambda)$ and $K(\lambda)$ are the incident light intensity and the sphere throughput efficiency, respectively, at a given λ, r is the reflection coefficient, and n is the number of reflections. Using for $x < 1$ the approximation

$$\sum_1^n x^n = \frac{1}{1 - x}$$

we get

$$I_0^m(\lambda) = K(\lambda) r I_0(\lambda) \frac{1}{1 - (1 - r)} = K(\lambda) I_0(\lambda)$$

therefore

$$I_t^m(\lambda) = K I_0(\lambda) \times [r + r(1 - r) + r(1 - r)^2 + \ldots + r(1 - r)^{n-1}] + T(1 - r)^n$$

and

$$T_n^m(\lambda) = I_t^m(\lambda)/I_0^m(\lambda) = r[1 + \sum_1^{n-1}(1 - r)^n] + (1 - r)^n T(\lambda)$$

solving for $T(\lambda)$ yields

$$T(\lambda) = \frac{T_n^m(\lambda) - r[1 + \sum^{n-1}(1 - r)^n]}{(1 - r)^n}$$

Using the approximation $(1 - r)^n \sim 1 - nr$ for $n \ll 1$ and neglecting all terms in r^2 and higher powers

$$T(\lambda) = \frac{T_n^m(\lambda) - nr}{1 - nr}$$

References

Bakker, E. P., Rottenberg, H., & Caplan, S. R. (1976) *Biochim. Biophys. Acta 440*, 557–572.

Becher, B., & Cassim, J. Y. (1976) *Biophys. J. 16*, 1183–1200.

Becher, B., & Ebrey, T. G. (1977) *Biophys. J. 17*, 185–191.

Belyakova, T. N., Kadzyauskas, Yu. P., Skulachev, V. I., Smirnova, I. A., Chekulayeva, L. N., & Yasaytis, A. A. (1975) *Dokl. Akad. Nauk SSSR 223*, 483–486.

Bevington, R. P. (1969) *Data Reduction and Error Analysis*, McGraw-Hill, New York.

Bogomolni, R. A. (1977) *Fed. Proc., Fed. Am. Soc. Exp. Biol. 36*, 1833–1839.

Bogomolni, R. A., Baker, R. A., Lozier, R. H., & Stoeckenius, W. (1976a) *Biochim. Biophys. Acta 440*, 68–88.

Bogomolni, R. A., Lozier, R. H., & Stoeckenius, W. (1976b) *Biophys. J. 16*, 21a.

Danon, A., & Caplan, S. R. (1976) *Biochim. Biophys. Acta 423*, 133–140.

Dencher, N., & Wilms, M. (1975) *Biophys. Struct. Mech. 1*, 259–271.

Drachev, L. A., Kaulen, A. D., & Skulachev, V. P. (1977) *FEBS Lett. 87*, 161–167.

Duysens, L. N. M. (1956) *Biochim. Biophys. Acta 19*, 1–12.

Eisenbach, M., Garty H., Bakker, E. P., Klemperer, G., Rottenberg, H., & Caplan, S. R. (1978) *Biochemistry 17*, 4691–4698.

Goldschmidt, C. R., Ottolenghi, M., & Korenstein (1976) *Biophys. J. 16*, 839–843.

Goldschmidt, C. R., Kalisky, O., Rosenfeld, T., & Ottolenghi, M. (1977) *Biophys. J. 17*, 179–183.

Hartmann, R., & Oesterhelt, D. (1977) *Eur. J. Biochem. 77*, 325–335.

Hartmann, R., Sickinger, H. D., & Oesterhelt, D. (1977) *FEBS Lett. 82*, 1–7.

Hatchard, C. G., & Parker, C. A. (1956) *Proc. R. Soc. London, Ser. A 235*, 518–536.

Hess, B., Korenstein, R., & Kuschmitz, D. (1978) in *Energetics and Structure of Halophilic Organisims* (Caplan, S. R., & Ginzburg, M., Eds.) pp 89–108, Elsevier/North-Holland Publishing Co., Amsterdam.

Hwang, S.-B., & Stoeckenius, W. (1977) *J. Membr. Biol. 33*, 39–42.

Kayushin, L. P., & Skulachev, V. P. (1974) *FEBS Lett. 39*, 39–42.

Kelly, M., Norgard, S., & Liaaen-Jensen, S. (1970) *Acta Chem. Scand. 24*, 2169–2182.

Kung, M. C., Devault, D., Hess, B., & Oesterhelt, D. (1975) *Biophys. J. 15*, 907–911.

Lanyi, J. K., & MacDonald, R. E. (1976) *Biochemistry 15*, 4608–4614.

Lee, J., & Seliger, H. H. (1964) *J. Chem. Phys. 40*, 519–523.

Lozier, R. H., & Niederberger, W. (1977) *Fed. Proc., Fed. Am. Soc. Exp. Biol. 36*, 1805–1809.

Lozier, R. H., Bogomolni, R. A., & Stoeckenius, W. (1975) *Biophys. J. 15*, 907–962.

Lozier, R. H., Niederberger, W., Bogomolni, R. A., Hwang, S.-B., & Stoeckenius, W. (1976) *Biochim. Biophys. Acta 440*, 545–556.

Lozier, R. H., Niv, H., Hwang, S.-B., Havel, P., Bogomolni, R. A., & Stoeckenius, W. (1979) *Biophys. J. 25*, 77a.

MacDonald, R. E., & Lanyi, J. K. (1975) *Biochemistry 14*, 2882–2889.

Michel, H., & Oesterhelt, D. (1976) *FEBS Lett. 65*, 175–178.

Oesterhelt, D. (1975) *Ciba Found. Symp. 31*, 147–167.

Oesterhelt, D., & Hess, B. (1973) *Eur. J. Biochem. 37*, 316–326.

Oesterhelt, D., & Krippahl, G. (1973) *FEBS Lett. 36*, 72–76.

Oesterhelt, D., & Stoeckenius, W. (1973) *Proc. Natl. Acad. Sci. U.S.A. 70*, 2853–2857.

Ormos, P., Dancshazy, Zs., & Karvaly, B. (1978) *Biochim. Biophys. Acta 503*, 304–315.

Ort, D., & Parson, W. (1978) *J. Biol. Chem. 253*, 6158–6164.

Ort, D., & Parson, W. (1979) *Biophys. J. 25*, 341–353.

Rabinowitch, E. (1964) in *Photosynthesis*, Academic Press, New York.

Renthal, R., & Lanyi, J. K. (1976) *Biochemistry 15*, 2136–2143.

Stoeckenius, W., Bogomolni, R. A., & Lozier, R. H. (1975) in *Molecular Aspects of Membrane Phenomena* (Kaback, H. R., Neurath, H., Radda, G. K., Schwyzer, R., & Wiley, W. R., Eds.) pp 306–315, Springer-Verlag, New York.

Stoeckenius, W., Lozier, R. H., & Bogomolni, R. A. (1979) *Biochim. Biophys. Acta 505*, 215–278.

Wagner, G., & Oesterhelt, D. (1976) *Ber. Dtsch. Bot. Ges. 89*, 289–292.

Wraight, C. A., & Clayton, R. K. (1973) *Biochim. Biophys. Acta 333*, 246–260.